

# Experimental and Numerical Study of a Loaded Cylindrical Glass Fiber-Reinforced PA6 Gear

J. Cathelin, M. Guingand, JP. de Vaujany and F. Ville

## Introduction

Polymer gears find increasing applications in the automotive industry, office machines, food machinery, and home appliances. The main reason for this success is their low cost. Their low weight, quietness of operation, and meshing without lubricant are also interesting. However, they have poor heat resistance and are limited to rotational transmission. In order to improve the gears' behavior, glass fiber is added, where their lower cost and higher strength—compared to un-reinforced polymers—offers a potential increase in the gears' performance (Refs. 1–2).

Most of the literature on fiber-reinforced plastic gears is based on experimental studies. These last cover various aspects of plastic-reinforced gear pairings, including several studies on wear behavior (Refs. 3–4), working temperature (Refs. 5–6), failure modes (Refs. 2 and 7), and fiber orientation and its influence on gear metrology (Ref. 8).

In order to reduce the development costs, and particular to reduce validations testing under actual conditions, numerical models are developed. Due to the relative complexity of plastic material, very few numerical models exist. In fact, polymer behavior is viscoelastic (Ref. 9), which means that it depends on loading duration, temperature, and, for some polymers such as polyamide—on humidity. Moreover, fiber-reinforced gears have an anisotropic behavior.

Tsai and Tsai (Ref. 10) realized the first computing studies on static transmission errors as a result of an elastic multi-tooth contact FEM (Finite Element Method) analysis. More recently, Lin and Kuang (Ref. 11) developed a dynamical model for the case of Polyamide 6.6 and POM plastic gears. Their approach is based on a full FEM that incorporates the effects of position-varying tooth mesh stiffness, damping ratio, load sharing, tooth profile wear, and temperature on dynamic contact load.

However, the accuracy of the results given by such an approach is largely counterbalanced by very time-consuming calculations.

To estimate the load sharing, the LaMCoS laboratory has developed an approach that consists in solving the displacement compatibility equation. The quasi-static model uses the influence coefficients method, which requires low computational time. This method has been applied on cylindrical gears (Ref. 12), face gears (Ref. 13) and spiral bevel gears (Ref. 14) of elastic materials. Recently, Hiltcher et al. (Ref. 15) adapted the method developed by LaMCoS for metal worm gears to the case of a plastic wheel and steel worm. Then in 2009, Letzelter et al. (Ref. 16) have developed a quasi-static load sharing model in the case of Polyamide 6.6 cylindrical gears. This method takes into account the viscoelastic behavior with a generalized Kelvin-Voigt model, and provides contact pressure, stress in the tooth roots and transmission error. This method has the advantage of being much less time-consuming, while also taking into account temperature and rotational speed effects. Following these developments, this study presents a similar method adapted for fiber-reinforced polyamide gears.

The work presents the thermal behavior of polyamide 6+30% glass fiber and the validation of the numerical model by measuring the loaded transmission error; which can be expressed as the phase difference of the driven gear compared to its theoretical position given by the transmission ratio. This is one result that is global enough to validate the three steps of the model: geometry, kinematics and load sharing. The measurements are carried out on a test bench developed at the LaMCoS laboratory (Ref. 17) using optical encoders to measure the angular positions of the pinion and the gear and an infrared thermal camera to measure the working temperature.

## Generality on PA6+30%GF Gears

### Gear geometry and molding conditions.

Reinforced polyamide 6 with 30% glass fiber granules was used to mold the gears. Polyamide 6 has a semi-crystalline structure, a glass temperature transition of 60°C, and a fusion temperature of 220°C at 0% relative humidity. Table 1 presents the gear's data.

In this study, a disc gating solution (Fig. 1) is used that has the best filling and fiber orientation regularity. The cavity geometry, molding conditions, and cooling conditions are obtained thanks to standard commercial molding process simulation software.

**Fiber orientation.** The fiber orientation and distribution in an injection-molded part is a function of component geometry; molding conditions (gating, temperature, pressure and holding time); matrix material; polymer melt viscosity; and fiber type (aspect ratio, density and volume fraction) (Ref. 18). Fiber orientation is obtained through molding process simulations and tomography microscopy observations (Ref. 19). Comparisons between quantitative, simulated fiber orientation predictions and the qualitative tomography observations show similar trends. Three main fiber organization areas were defined; each section is represented in Figure 2.

On the flank area, fibers tend to be parallel to the surface. In the core zone, they are more vertical, and near the tooth root, the orientation is more anisotropic. This model, taking into account the real fiber orientation, was later implemented in standard FEM simulation software.

**Gear metrology.** In real conditions, mold shrinkage varies with part thickness, mold layout, processing conditions and mold temperature (Ref. 20). During injection molding of fiber-reinforced polymers, the incorporation of fibers causes a significant effect on linear shrinkage. The asymmetric, ridged nature of the glass fibers restricts shrinkage of the polymer matrix in the fiber orientation direction, while the direction perpendicular to that shows lower shrinkage than the base polymer (Ref. 20). Senthilvelan et al. (Ref. 8) show an increase in involutes profile form deviation among polyamide 6.6 fiber-reinforced gears when

Table 1 Gear data		
	Pinion	Gear
Module (mm)	3	3
Pressure angle (°)	20	20
Number of teeth	32	41
Tooth width (mm)	20	20
Addendum coefficient	0	0

compared to homogeneous polyamide 6.6 gears.

Shrinkage creates profile deviation and run out, which correspond to the eccentricity of the gear teeth. Both parameters have a strong influence on the transmission error. Gear tooth profile and lead deviations were measured on three teeth, which are equally spaced. If there is not deviation, the theoretical and measured traces would be superposed. The involutes profile was measured from the tip circle diameter to base circle diameter.

The fiber orientation shrinkage effect was taken into account by standard commercial molding process simulation software, although form deviation is also observed. The measurements show an increase of thickness near the tooth top of the pinion and wheel. This derives from an over-estimation of the shrinkage value in the mold cavity. Conical shape on the pinion and the wheel was also observed (Fig. 3); this is supposed to come from a differential cooling during part ejection.

The maximum involute profile form deviation in a reinforced polyamide 6 gear are 82 μm (ISO 1328 Quality 12) for the pinion and 54 μm (ISO Quality 11) for the wheel. Tooth profile modification, in relation with the metrology results, was implemented in the load sharing simulation software developed by the LaMCoS laboratory.

## Numerical Model

The numerical model is based on the procedure developed for steel and polyamide 6.6 gears; this procedure is divided into the three principal steps (Ref. 21). Initially, tooth geometry is obtained with tooth corrections adapted to molded gears. The second step consists of an unloaded kinematics simulation to determine the potential contact zones, while the load sharing between all the teeth in contact is computed in the last step. When torque is applied for each quasi-static position, the instantaneous pressure distribution can be

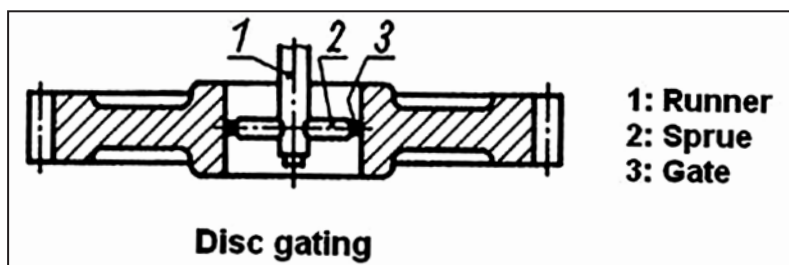


Figure 1 Gating location.

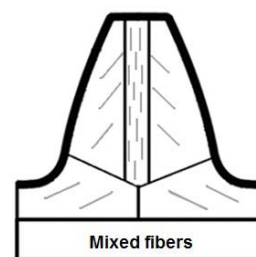


Figure 2 Fibers distribution outline.

For Related Articles Search

plastic gears

at www.geartechnology.com

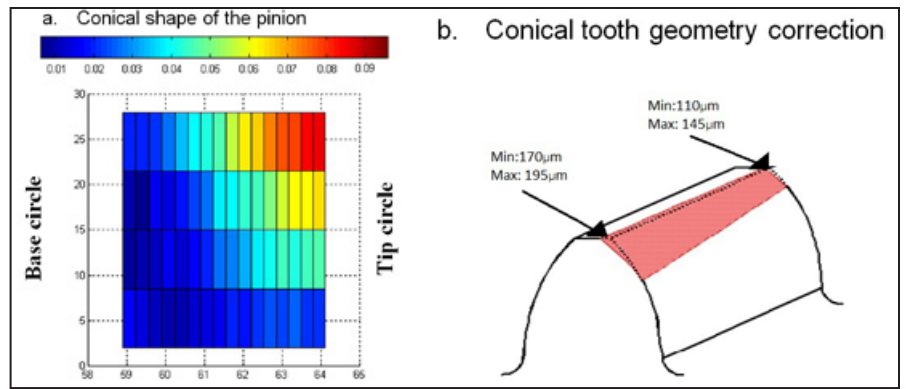


Figure 3 Conical shape.

estimated for all the teeth in contact simultaneously. Finally, it is possible to calculate the meshing stiffness, the stress in the tooth roots, and the loaded transmission error. The third step integrates the viscoelastic displacement and the loading history in the case of PA6+30% GF material.

Steps 1 and 3 must be modified for the gears made of PA6+30% GF materials. In step one the geometry — due to the shrinkage presented on Figure 3 — was integrated. In step 3 a new behavior model based on the method proposed by Letzelter et al. (Ref.16) for a homogeneous polyamide 6.6 was developed.

**Mechanical behavior of polyamide 6+30% GF.** A description of the viscoelastic properties of polyamide 6+30% GF comes from a generalized Kelvin-Voigt model (Fig.4). The main differences consist of adding the elastic behavior of the fiber into the displacement model and integrating their

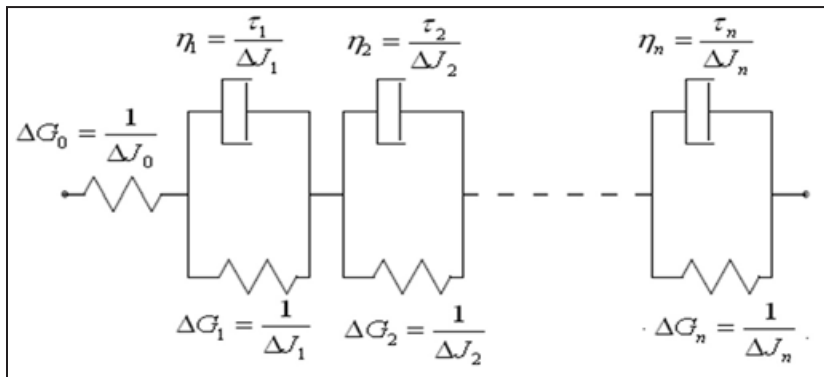


Figure 4 Generalized Kelvin model.

anisotropic organization. The generalized Kelvin-Voigt method takes into account the viscoelastic behavior of polymer and establishes a relation between the temporal displacement and the total strain. For a sample of  $l$  length, the global displacement at instant  $t$ ,  $u(t)$  is obtained with Equation 1:

$$u(t) = l \cdot \sigma(t) \sum_{i=0}^n \Delta J_i \left( \frac{dt}{dt + \tau_i} \right) \cdot l \cdot \sum_{i=0}^n u^i(t-dt) \left( \frac{\tau_i}{dt + \tau_i} \right) \quad (1)$$

Where  $\sigma(t)$  is the stress level,  $\tau_i$  and  $u^i$  respectively, the retardation time and displacement of a block  $i$  in the generalized Kelvin model, and  $n$  is the number of blocks. Relation (Ref.1) is used to solve the load sharing problem in the third step of the process. First, it is necessary to determine the viscoelastic properties  $\Delta J_i$  and  $\tau_i$ . These values are determined with DMA (Dynamical Mechanical Analysis) tests at different frequencies, temperatures and humidity ranges.

**Load sharing model.** The method to solve the instantaneous load sharing is based on a unique process used for all types of gears made with steel or steel/polymer materials. The final displacement at a node is obtained through the combination of the equations of displacement compatibility and torque equilibrium. The influence coefficients methods (Ref.22) solve this multi-contact problem.

In the case of plastic gear, it is necessary to know the loading history and displacements of the gear and pinion. Consequently, the local meshing on the contact zone developed for polymer gears is different from those developed for steel gears.

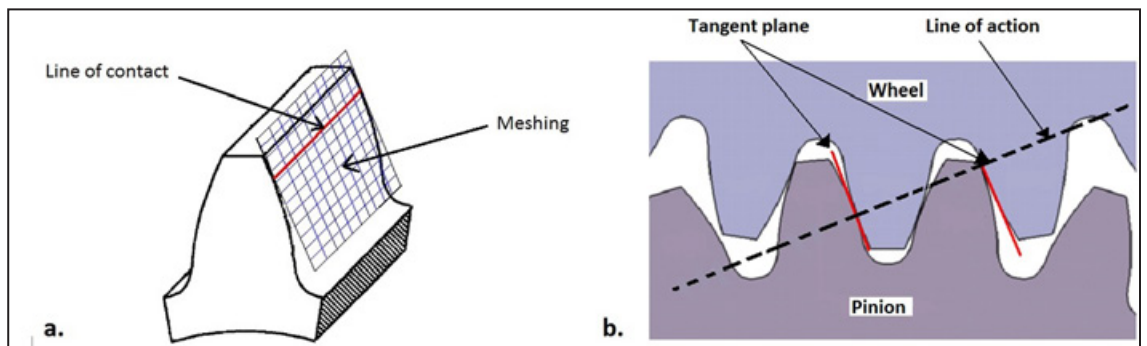


Figure 5 Local meshing on the contact zone.

The surface is larger than the latter, and covers the entire tooth surface (Fig. 5). Thus, for a kinematics position, it is possible to save the displacement of the pinion and the gear for computing the next kinematics position. This is done to account for the displacement history, which is needed to compute the viscoelastic behavior of the polyamide 6+30% GF material.

#### The equation of compatibility of displacement.

The load sharing problem consists of solving the equations of displacement compatibility (Eq. 2) and driving torque (Eq. 3) to balance the torque.

$$p(M_k).e(M_k) = p(M_k).(\delta(M_k) + u(M_k) - \alpha) = 0 \quad (2)$$

$$C_{motor} = \sum_{k=1}^K (p_k s_k \vec{n}_k \wedge \vec{M}_k) \quad (3)$$

With  $K$  is the number of nodes of the meshing,  $p(M_k)$  is the contact pressure at point  $M_k$ ,  $e(M_k)$  is the gap between the profiles of the gear and pinion at point  $M_k$  after the loading,  $\delta(M_k)$  is the gap between the profiles of the gear and pinion at point  $M_k$  before the loading,  $u(M_k)$  is the displacement at point  $M_k$  and  $\alpha$  is the global body adjustment. In Equation 3,  $s_k$  is the contact surface around the point  $M_k$  and  $\vec{n}_k$  a perpendicular vector to the tangent plan.

**The influence coefficient.** In order to solve the load sharing problem, it is necessary to compute the displacement  $u_k$ , depending on pressure  $p_k$ . It is possible to write the relation (4) between the displacement and the pressure with the method of the influence coefficients. There are 2 types of influence coefficients:

- Bulk influence coefficients  $C_{kj}^V$  computed by finite element method. This method is applied on three teeth to deduct the effect of local displacement on the neighboring teeth. Moreover, the finite element method is based on Figure 2, where the fiber presence and its orientation are taken into account.

- Surface influence coefficients  $C_{kj}^S$  computed with Boussinesq theory (Ref. 23).

$$u_k = \sum_{j=1}^K C_{kj} p_j \text{ with } C_{kj} = C_{kj}^V + C_{kj}^S \quad (4)$$

However, regarding the relation (Eq. 4) proposed for steel gears — in the case of polymer gears, the bulk influence coefficient is defined by the relation (Eq. 5). The geometrical influence coefficient is not linked with the polyamide 6 matrix compliance; it only depends on the geometry and fiber orientation, where  $J_{mat}$  is the compliance of the polyamide (inverse of the Young modulus). This distinction could be made because of the pure elastic behavior of the glass fiber and its non-influence on the viscoelastic behavior of the polyamide 6 matrix (Ref. 19).

$$C_{kj}^V = J_{mat} C_{kj}^{V*} \quad (5)$$

$$C_{kj}^S = J_{mat} C_{kj}^{S*} \quad (6)$$

$C_{kj}^{S*}$  in relation

Equation 6 represents the surface geometrical influence coefficient non-dependent on the material's compliance, but dependent of the fibers' presence. Fibers are presumed purely parallel to flanks in the case of the surface influence coefficient.

**The viscoelastic displacement on meshing.** The displacement in Equation 1 is combined with the influence coefficient method. The Kelvin-Voigt parameters correspond to the polyamide 6 matrix behavior.  $\tau_i$  and  $\Delta J_i$  remains the same for the surface and bulk material with the assumption that fiber doesn't affect the viscoelastic behavior of the polyamide 6 matrix (Ref. 19).

$$u_k(t) = \sum_{i=1}^n u_k^i(t) \quad (7)$$

$$u_k^i(t) = \sum_{j=0}^n \left[ C_{kj}^{*V} p_j(t) \Delta J_i \left( \frac{\Delta t}{\tau_i + \Delta t} \right) + C_{kj}^{*V} p_j(t) \Delta J_i \left( \frac{\Delta t}{\tau_i + \Delta t} \right) \right] + u_k^i(t-dt) \left( \frac{\Delta t}{\tau_i + \Delta t} \right) \quad (8)$$

$k$  is the index of the meshing nodes and  $p_j(t)$  the contact pressure at point  $j$ .  $u_k^i(t-dt)$  represents the history of displacements caused by the load at time  $t-dt$ . Fiber orientation is taken into account through  $C_{kj}^{*S}$  regarding the surface displacements where fibers are assumed parallel to the surface.  $C_{kj}^{*V}$  integrate the fiber influence regarding the bulk displacements.

The system of equations, which includes the relations Eqs. 2, 3 and 8, is used to calculate the load sharing. This is achieved by using a fixed-point algorithm. It is also necessary to create a history of the displacements. To obtain this one, the displacement and the load sharing are calculated for two teeth situated just before they come into contact.

**Thermal model.** According to several studies, plastic gears have an important temperature increase during running (1). This temperature has an impact on the viscoelastic behavior of the material.

In the case of polymers with rolling contact, Koffi et al. (Ref. 24) show that the friction energy is much more important than the polymer's internal energy. Following the results of the study conducted by Koffi et al. (Ref. 24), Mao (Ref. 25) and Hooke et al. (Ref. 26), the viscoelastic warming can be neglected, compared to the friction warming. Erhard et al. (Ref. 27) defined the bulk temperature variation as a thermal balance between the heating generation  $Q_1$  by friction and loss through the room temperature convection  $Q_2$ .

$$Q_1 = 2,6.P.\mu.\frac{i_u + 1}{z_1 + 5.i_u} \quad (9)$$

$$Q_2 = A_1.\alpha_w.(T_{Zi} - T_u) \quad (10)$$

Where  $P$  is the power brought by the motor,  $\mu$  the friction coefficient,  $i_u$ , the transmission ratio,  $z_1$ , the number of teeth of the pinion,  $A_1$ , a geometrical coefficient related to the thermal exchange on the surface of the concerned gear,  $\alpha_w$ , a thermal convection coefficient of the concerned gear,  $T_{Zi}$  concerned gear temperature, and  $T_u$  the room temperature. The thermal balance between Equations 9–10 lead to the gear bulk temperature (Eq. 11).

$$T_{Zi} = T_u + P.\mu.f_{ED}.136.\frac{i_u + 1}{z_1 + 5.i_u} \left[ \frac{k_2.171000}{b.z_i.(V_x.m)^{0.75}} \right] \quad (11)$$

Where  $f_{ED}$  is related to the meshing duration,  $V_x$  rotating speed at the top radius,  $m$  the module,  $b$  the gear width,  $k_2$  coefficient depending on the gear material couple.

A flash temperature model that estimates the maximal surface temperature variation on a gear tooth flank has been developed by Block (Ref. 28) and Erhard et al. (Ref. 27). This temperature increase is intended to be over an insufficient period of time to locally modify the polyamide 6 contact behavior. For this reason the flash temperature effect on contact displacements is not taken into account for the following model. The polyamide 6+30%GF temperature can be expressed as:

$$T_{max} = T_{Amb} + \Delta T_{Bulk} \quad (13)$$

The temperatures (Equation (13)) are then integrated in the load sharing model together with the humidity rate through modifying the relaxation time  $\tau_i$ .



**Thermal expansion.** Thermal expansion of polyamide is 3 times higher than steel, and room humidity has an influence on the gear geometry as well. W. Kraus (Ref.29) proposed the Equation 12 to establish a link between the module and the thermal and humidity expansion effect.

$$m' = m.[1 + \alpha_T.(T_{Zi}-T_u) + \Delta d'.g] \quad (12)$$

Where  $m$  is the original gear module,  $\alpha_T$  the thermal expansion coefficient,  $T_{Zi}$  corresponds to the room temperature,  $T_u$  the original room temperature,  $\Delta d'$  the humidity expansion coefficient depending on the exposure time and humidity rate,  $g$  is a parameter linked to polymer type.

A numerical study taking into account the expansion effect was conducted on the gear data in Table 1 and shows its influence on transmission error.

The expansion coefficient of the polyamide 6+30%GF is approximate by a rule of mixture  $\alpha = 27.3 \times 10^{-6}$ . A backlash of 0.2 mm was used according to the mounting condition proposed by Boyer (Ref.30). In both cases, with and without Table 2, the expansion effect was simulated. Three parameters were observed—maximal tooth root stress, maximal contact pressure on the pitch circle and transmission error at two different bulk temperatures, 40°C and 80°C. At 40°C, the gear module supposed to be  $m = 2.998$  mm and at 80°C,  $m = 3.002$  mm.

Results from Table 2 show a slight influence of the thermal expansion on flank pressure and tooth root stress. Nevertheless, a difference of 18%

is observed on the transmission error amplitude. Therefore the expansion effect can't be neglected.

### Experimental Measurements

**Testing device.** An experimental test bench has been developed by the LaMCoS laboratory. The original characteristic of this bench is the instantaneous measurements of the thermal behavior, done by an infrared camera, and the transmission error; Figure 6 shows a view of the experimental system.

The asynchronous motor (Ref. 1) is powered by a variable speed drive. The mechanical power created by the electrical motor is transmitted by a belt to the rotating shaft of the pinion. The shafts are supported by four plain bearings to limit the dynamical effects. A powder brake (Ref.2) mounted on the rotation axis of the gear creates a torque. The infrared camera (Ref.3) is clamped on an original system, able to capture images closed to the tooth meshing in the transverse plane (Ref.17). Two optical encoders (Ref.4) are placed on each rotating shaft. The experimental device is fixed on a heavy base plate, and the electrical motor and the support of the infrared camera are clamped on rubber pads.

### Transmission error measurements

**Transmission error measurements principle.** The angular positions of the pinion and gear that give the transmission error are measured with optical encoders directly clamped on the rotating shaft;

**Table 2 Results without and with thermal expansion (TE)**

	Average Transmission error [mrad]		Transmission error amplitude [mrad]		Flank pressure [MPa]		Tooth root stress [MPa]	
40°C without TE	0.637		0.299		30		9.40	
80°C without TE	1.269		0.310		23		8.82	
40°C with TE	0.649	1,9%	0.329	10%	30.5	1.6%	9.3	0,2%
80°C with TE	1.251	1,4%	0.255	18%	22.5	2.1%	8.4	0,6%

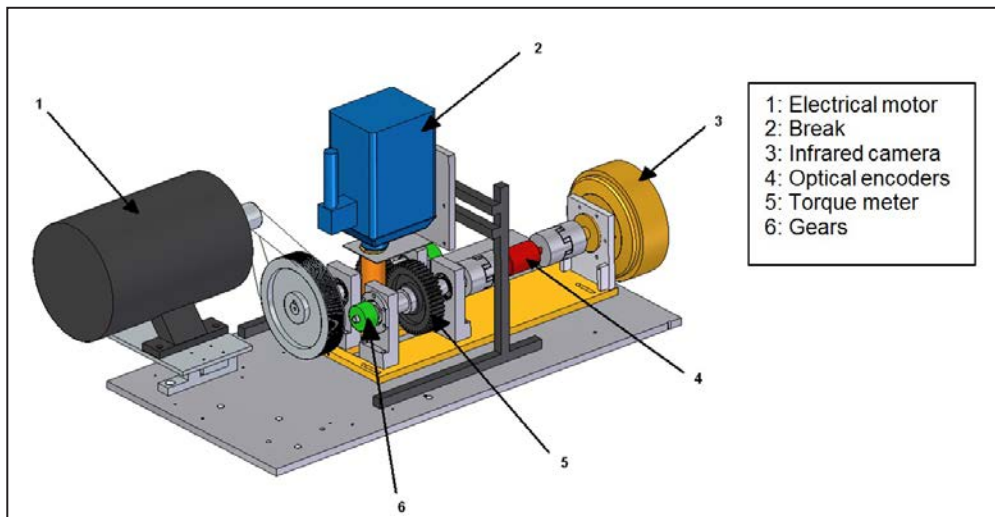


Figure 6 Perspective scheme of the test bench.

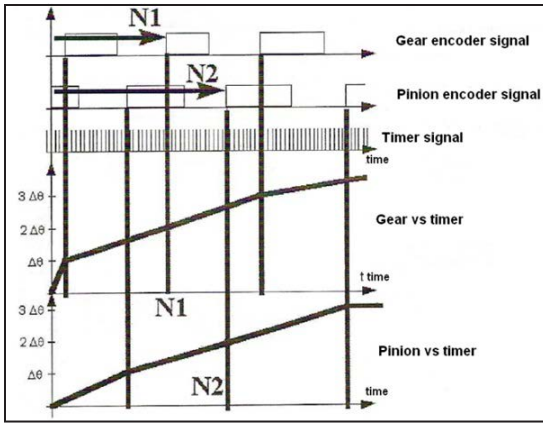


Figure 7 Phase difference encoder (Ref. 14).

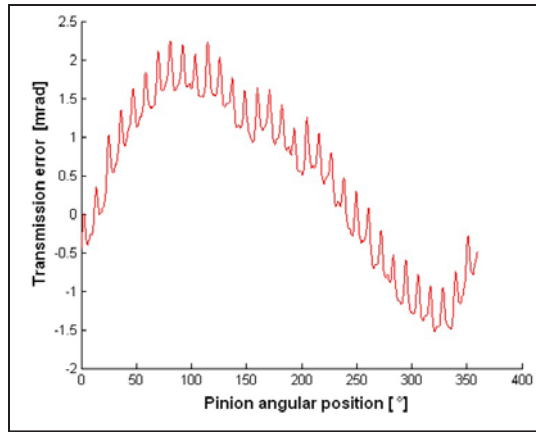


Figure 8 Transmission error on one gear revolution.

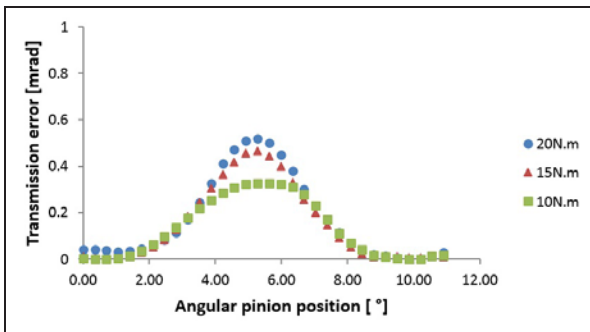


Figure 9 Influence of the torque at 50 rpm.

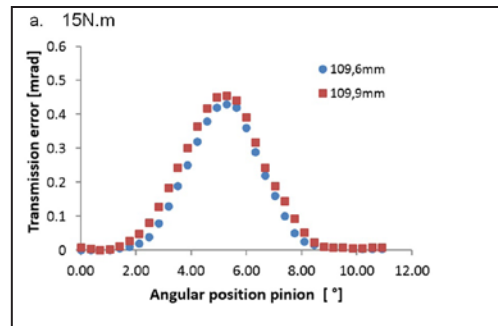


Figure 10 Reference cases at 50 rpm, 20 N.m.

these components measure the transmission error. The principle of this measurement is based on counting pulses delivered by a timer at a very high frequency (80 MHz) between two rising edges of the signal delivered by the optical encoders. This time-counting method must be carried out simultaneously on the two signals with the same reference (Fig. 7, i.e. — the same timer and counter). Then, the time evolution of the pinion and the gear angular positions are defined with a sampling rate given by the number of pulses on each encoder.

The signal of the transmission error is built using the two laws of angular evolution of the encoders. (See the gear and pinion vs. time law curves evolution on Fig. 7). This angular measurement method consists of performing the calculation at the rising edge — either on the pinion signal (pinion rising edge) or on the gear signal (gear rising edge). The transmission error can be given as an angular displacement on either the pinion or gear shaft. In the presented study, the gear shaft angular error is given at a stabilized speed. The principle is based on the timer signal counting between the encoder rising edge.

The numerical treatments of the results are achieved in three main steps:

In the first step, the transmission error measurement is built on a single pinion revolution. The pinion has 32 teeth that correspond to 32 different transmission errors (Fig. 8). The main oscillation, with a 4 mrad amplitude on Figure 8, corresponds to the eccentricity of the shaft.

Second step: to avoid the effect of eccentricity, which is not taken into account in the simulation model, the transmission error on a single gear revolution is sampled in 32 pieces. One sample corresponds to one tooth meshing.

The third step consists of computing the average transmission error on each sample.

**Transmission error measurement results.** The tested gears data is presented in Table 1. The tests were carried out at low speed in order to conform to the quasi-static conditions. Figure 9 presents the torque influence at 50 rpm. A good agreement regarding the shape of the curve is found with the simulation results presented (Fig. 10).

Figure 10 corresponds to the reference cases used for the numerical validation. Four cases are used at two torque levels and for two center distance values. We can notice that an increase of center distance leads to a slightly higher transmission error (Fig. 10).

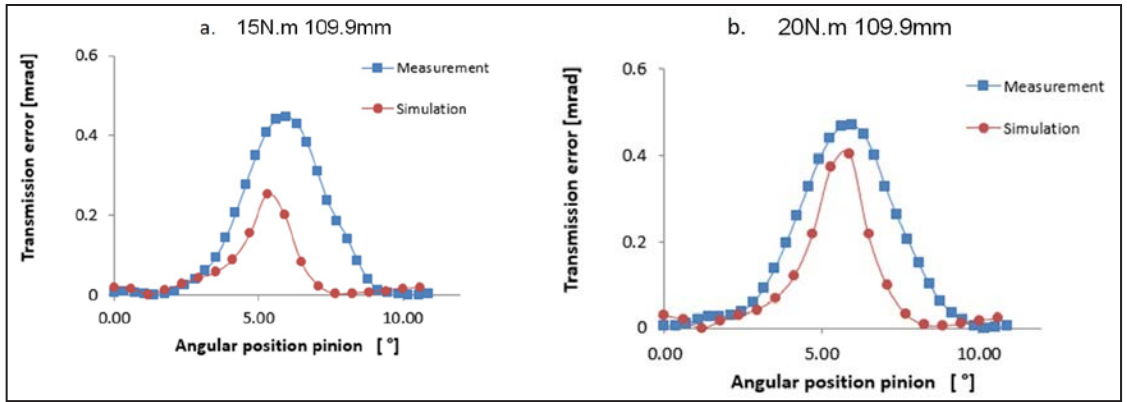


Figure 11 Transmission error comparison without tooth modifications.

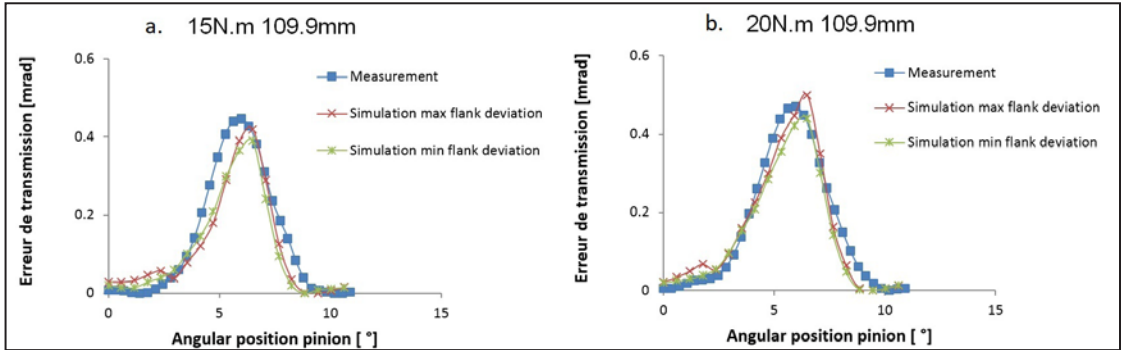


Figure 12 Transmission error comparison with tooth tip relief modifications.

On Figure 11, simulations are carried out on a single tooth meshing, which represents one transmission error period, at 19°C and 40% relative humidity; these conditions are close to the glass temperature. Reference case “measurement” — with simulation results, and without geometrical tooth modification — are compared. Similar trends are observed, but the gap between the simulated results and measured one remain important.


On Figure 12, tooth modifications on the pinion and wheel have been implemented as previously described. Two simulation cases are presented — one taking into account the highest geometrical deviation measure on the gear flank, whereas the other is taking into account the lowest geometrical deviation. Better agreements between simulation and measured results are observed. Transmission error amplitude difference remains below 10%.

### Conclusion

The presented numerical model simulates the loaded behavior of polyamide 6+30% GF gears obtained by injection molding. It is based on three main steps: definition of real tooth geometry, kinematics simulation, and calculation under load. The latter step is used to calculate the load sharing

between the teeth and also the transmission error.

Numerical investigation on thermal expansion shows that its effect on transmission error is not negligible. A thermal model taking into account the working conditions to predict the gear temperature was implemented. The simulation and measurement results are used to validate the model. Experimental validations are carried out on a test rig, by measuring the loaded transmission error with two optical encoders. The measurement is based on the angular evolution of the sensors and their phase differences. Results are then filtered on one tooth meshing to remove the eccentricity effects.

At first, similar curve shapes are obtained, but an important difference of amplitude is observed. A better correlation is obtained while implementing the tooth profile correction according to the measurement on molded gears. The next step of the study will focus on the validation of this model on a broader range of spur, as well as helical gear size and, eventually, plastic-metal pairing. 

**Acknowledgements.** *The authors thank the French Research Ministry for its financial support MESR.*

**For more information:** Questions or comments regarding this paper? Contact Julien Cathelin at [julien.cathelin@gmail.com](mailto:julien.cathelin@gmail.com).

## References

- Senthilvelan, S. and R. Gnanamoorthy. "Effect of Rotational Speed on the Performance of Unreinforced and Glass Fiber-Reinforced Nylon 6 Spur Gear," *Material and Design*, 28, 2007, pp.765–772. Doi: 10.1016/j.matdes.2005.12.002.
- Crippa, G. and P. Davoli. "Comparative Fatigue Resistance of Fiber-Reinforced Nylon 6 Gears," *ASME Journal of Mechanical Design*, 1995, 117, pp.193–198. Doi: 10.1115/1.2826106.
- Feulner, R. Verschleiss trocken laufender Kunststoffgetriebe-Kennwertermittlung und Auslegung, Ph.D. thesis, University of Erlangen, Germany, 2008.
- Kurokawa, M., Y. Uchiama, et al. "Performance of Plastic Gear Made of Carbon-Reinforced Polyamide 12," *Wear*, 2003, 254, pp.468–473. Doi: 10.1016/S0043-1648(03)00020-6.
- Hooke, C.J. "Measurement and Prediction of the Surface Temperature in Polymer Gears and its Relationship to Gear Wear," *ASME Journal of Tribology*, 1993, 115, pp.119–124. Doi: 10.1115/1.2920964.
- Erhard, G. and C. Weis. Zur Berechnung der Zahn- und Flankentemperatur von Zahnradern aus Polymerwerkstoffen, Konstruktion, 1987, 39, pp.423–430.
- Senthilvelan, S. and R. Gnanamoorthy. "Damage Mechanism in Injection Molded Unreinforced, Glass and Carbon-Reinforced Nylon 66 Spur Gears," *Applied Composite Materials*, 2004, 11, pp.377–397. Doi: 10.1023/B:ACMA.0000045313.47841.4e.
- Senthilvelan, S. and R. Gnanamoorthy. "Influence of Reinforcement on Composite Gear Geometry," *Mechanism and Machine Theory*, 2008, 43, pp.1198–1209.
- Moriwaki I., K. Tada, F. Tokuda, G.D. Hui and K. Saito. "Viscoelastic Behavior of Plastic Gears for Power Transmission — Fundamental Investigation," *7th International Power Transmission and Gear Conference*, 1996, pp.125–131.
- Tsai, M.H and Y.C. Tsai. "A Method for Calculating Static Transmission Errors of Plastic Spur Gears Using FEM Evaluation," *Finite Elements in Analysis and Design*, 1997, 27, pp.345–357. Doi: 10.1016/S0168-874X(97)81968-3.
- Lin, A. and J. Kuang. "Dynamic Interaction between Contact Loads and Tooth Wear of Engaged Plastic Gear Pairs," *International Journal of Mechanical Sciences*, 2007, 50, pp.205–213. Doi: 10.1016/j.ijmecsci.2007.07.002.
- Guinand, M., J.P. de Vaujany and Y. Icard. "Fast 3-D Quasi-Static Analysis of Helical Gears Using the Finite Prism Method," *ASME Journal of Mechanical Design*, 2004, 126, pp.1082–1088. Doi: 10.1115/1.1798212.
- Guinand, M., J.P. de Vaujany and Y. Icard. "Analysis and Optimization of the Loaded Meshing of Face Gears," *ASME Journal of Mechanical Design*, 2005, 127, pp.135–143. Doi: 10.1115/1.1828459.
- de Vaujany, J.P., M. Guinand, D. Remond and Y. Icard. "Numerical and Experimental Study of the Loaded Transmission Error of a Spiral Bevel Gear," *ASME Journal of Mechanical Design*, 2007, 129, pp.129–135. Doi: 10.1115/1.2406089.
- Hiltcher, Y., M. Guinand and J.P. de Vaujany. "Load Sharing of a Worm Gear with a Plastic Wheel," *ASME Journal of Mechanical Design*, 2007, 129, pp.23–30. Doi: 10.1115/1.2359469.
- Letzelter, E., M. Guinand, J.P. de Vaujany and L. Chazeau. "Quasi-Static Load Sharing Model in the Case of Nylon 6/6 Cylindrical Gears," *Materials and Design*, 2009, 30, pp.4360–4368. Doi: 10.1016/j.matdes.2009.04.008.
- Letzelter, E., M. Guinand, M., J.P. de Vaujany and P. Schlosser. "A New Experimental Approach for Measuring Thermal Behavior in the Case of Nylon 6/6 Cylindrical Gears," *Polymer Testing*, 2010, 29, pp.1041–1051. Doi: 10.1016/j.polymertesting.2010.09.002.
- Weale, D.J., J. White and D. Walton. "The Effect of Fiber Orientation and Distribution on the Tooth Stiffness of a Polymer Composite Gear," *Proceedings of SPE Annual Technical Conference*, 1998, Atlanta.
- Cathelin, J., M. Guinand, J.P. de Vaujany and L. Chazeau. "Quasi-Static Load Sharing Model in the Case of Molded Glass Fiber-Reinforced Polyamide 6 Gears," *Applied Composite Materials*, 2015, 22, pp.343–362. Doi: 10.1007/s10443-014-9410-7.
- Beaumont, J.P., R. Nagel and R. Sherman. "Successful Injection Molding Process," *Design and Simulation*, Hanser Publishers, Munich, 2002. ISBN: 1569902917.
- Guinand, M., J.P. de Vaujany and C.Y. Jacquin. "Quasi-Static Analysis of a Face Gear Under Torque," *Computer Methods in Applied Mechanics and Engineering*, 2005, 194, pp.4301–4318. Doi: 10.1016/j.cma.2004.10.010.
- Teixeira Alves, J., M. Guinand and J.P. Vaujany. "Set of Functions for the Calculation of Bending Displacement for Spiral Bevel Gear Teeth," *Mechanism and Machine Theory*, 2010, 45, pp.349–363. Doi: 10.1016/j.mechmachtheory.2009.09.006.
- Boussinesq, J. Application des potentials à l'étude de l'équilibre et du mouvement des solides élastiques, Albert Blanchard, 1959, Paris.
- Koffi, D., R. Gauvin and H. Velle. "Heat generation in thermoplastic spur gears," *ASME Journal of Mechanics, Transmissions, and Automation in Design*, 1985, 107, pp.31–37. Doi: 0.1115/1.3258688.
- Hooke, C.J., K. Mao, D. Walton, A.R Breeds and S.N Kulkureka. "Measurement and Prediction of the Surface Temperature in Polymer Gears and its Relationship to Gear Wear," *ASME Journal of Tribology*, 1993, 115, pp.119–124. Doi: 10.1115/1.2920964.
- Mao, K. "A New Approach for Polymer Composite Gear Design," *Wear*, 2007, 262, pp.423–441. Doi: 10.1016/j.wear.2006.06.005.
- Erhard, G., C. Weis, H. Hachmann and E. Strickle. "Zur Berechnung der Zahn und Flankentemperatur von Zahnradern aus Polymerwerkstoffen, Konstruktion," 1987, 39, pp.423–430.
- Block, H. "Theoretical Study of Temperature Rise at Surface of Actual Contact Under Oiliness Lubricating Conditions," *Proc. Inst. Mech. Eng.*, 1937, 2, pp.222–235.
- Krause, W. "Flankenspiel bei Kunststoffzahnradern," *Antriebstechnik*, 2003, 42, pp.41–43.
- Boyer, A. "Transmission de puissance et engrenages en matière plastique," *Journée engrenages et transmissions ECAM, IET, CETIM*, 1990.

### Julien Cathelin

received his masters' degree at the National Institute of Applied Sciences, INSA of Lyon in 2010, specializing in mechanical and polymer material engineering. From 2010–2013 Cathelin taught mechanical engineering, structural dynamics at INSA Lyon before receiving his Ph. D in 2014 at the Contact and Structure Mechanics Laboratory, LaMCoS of the INSA Lyon; his thesis — "Mechanical Behavior Modeling of Fiber-Reinforced Polymer Cylindrical Gears." Cathelin is currently an engineer in the plastic materials industry.



### Jean-Pierre de Vaujany

is an associate professor (1997 to present) at the National Institute of Applied Sciences, INSA Lyon / Laboratory LaMCoS, where he teaches mechanical design and manufacturing. He also serves as director of the university's International Section Amerinsa.



### Michèle Guigand

is a senior associate professor (1991 to present) at the National Institute of Applied Sciences, INSA Lyon/ LaMCoS Laboratory, where she teaches courses in gear design and CADD. Her research field is gear design, i.e. — quasic-static model to optimize gear geometry regarding loaded behavior of spiral bevel gear, worm gear, pinion rack, face gear — made in metal or plastic material.



### Fabrice Ville

is a professor and researcher at INSA Lyon, where he is a member of the Mechanical Systems and Contacts research group.

